Supporting Online Material for

K^+ Channel Mutations in Adrenal Aldosterone-Producing Adenomas and Hereditary Hypertension

Murim Choi, Ute I. Scholl, Peng Yue, Peyman Björklund, Bixiao Zhao, Carol Nelson-Williams, Weizhen Ji, Yoonsang Cho, Aniruddh Patel, Clara J. Men, Elias Lolis, Max V. Wisgerhof, David S. Geller, Shrikant Mane, Per Hellman, Gunnar Westin, Göran Åkerström, Wenhui Wang, Tobias Carling, Richard P. Lifton*

*To whom correspondence should be addressed. E-mail: richard.lifton@yale.edu

Published 11 February 2011, *Science* **331**, 768 (2011)
DOI: 10.1126/science.1198785

This PDF file includes:

Materials and Methods

Subjects. Matched APA and venous blood DNAs were obtained from patients undergoing adrenalectomy for hypertension with primary aldosteronism and adrenocortical tumor at the Department of Surgery, University Hospital, Uppsala. Primary aldosteronism was diagnosed by a significantly elevated aldosterone:renin ratio (ARR), followed by confirmatory studies (*S1*). Renin was measured in 2 patients as plasma renin activity (PRA; in mg/L/hr) and in 20 patients as plasma renin concentration (PRC; in mIU/L). An elevated ARR was considered to be aldosterone:PRA or aldosterone:PRC ratio greater than 100 and 50, respectively; all APA patients had ARR > 230 (mean 420). Adrenal tumors were identified by CT scans. Adrenal vein sampling was usually performed in subjects over age 40 and documented lateralization of aldosterone production. When APA was considered the most likely diagnosis, unilateral adrenalectomy was performed (*S1*). All APAs were verified by histopathology. When it was determined that procurement of tissue for genetic studies was possible without compromising the histopathological diagnosis, tumor tissue, determined by microscopy to be free of normal adrenal tissue, was snap-frozen in OCT using liquid nitrogen and stored at -80ºC until nucleic acid extraction. All patients displayed postoperative normokalemia and improvement in blood pressure control. Subjects from kindred HPA1 were evaluated as previously described (*S2*). The research protocols of all studies were approved by local IRB's and informed consent was obtained from all participants.

DNA preparation, genotyping and exome sequencing. Genomic DNA was prepared from subject venous blood and tumor tissue by standard procedures. SNP genotyping of blood and

tumor genomic DNAs was performed on the Illumina Human 1M-Duo DNA Analysis BeadChip. The image data was analyzed and SNP genotypes were called using Beadstudio software (Illumina). Genome-wide intensity and B-allele frequency was plotted using a perl script.

Targeted capture of human whole exome sequences using solution-based 2.1M NimbleGen Exome array followed by Illumina Genome Analyzer IIx sequencing was performed as previously described (*S3*). Three lanes of paired-end sequence reads of 74 or 99 bp length were generated following the manufacturer's protocol. Subsequent image analysis and base calling was done by Illumina pipeline (ver. 1.5) with default settings at Yale University's High Performance Computing Cluster.

Genomic sequences were mapped to the human genome (hg18) using Maq software (*S4*). Reads aligned to the targeted sequences were retrieved and subjected to further analyses using perl scripts. Pairs of reads sharing the same start and end positions were regarded as PCR duplicates and discarded using Samtools software (*S5*). dbSNP (build 131) and 1000 genomes database (release 07/20/10) were used to test novelty of variations. For somatic mutation discovery, positions with at least 8 reads in both tumor and blood DNA were evaluated, and those with at least 2 minor allele calls in tumor and less than 5 minor allele calls in blood samples were further evaluated. The significance of differences in read distributions at these positions between tumor and blood were evaluated by two-tailed Fisher's exact test to produce a list of putative somatic mutations in tumors ranked by p-value. Under the assumption that few if any clonal somatic changes should occur in blood DNA, as a control the same test was applied to blood DNA using

tumor DNA as reference. Among the 4 tumor-blood pairs, there were 13 putative somatic mutations in tumor with $p < 10^{-4}$ vs. 1 putative somatic mutation in blood (which was not confirmed), consistent with a high fraction of the variants in tumor representing *bona fide* somatic mutations. In contrast, the number of putative somatic mutations was similar in tumor and blood for $p > 10^{-4}$ (fig. S2). Consistent with expectation from this analysis, 12 of 13 putative somatic mutations in tumor with $p < 10^{-4}$ validated by Sanger sequencing while 0 of 28 with $10^{-3} > p > 10^{-4}$ validated (table S3). To evaluate the somatic mutation rate we considered all bases with at least 40 independent Illumina reads, which comprised 86.2% of the targeted bases in tumors. We also assessed small LOH segments (down to 1 Mb) and did not find any small somatic LOH segments in any of the 4 tumors subjected to exome sequencing.

Direct Sanger sequencing of putative somatic mutations identified by exome sequencing and of *KCNJ5* in all tumor-blood pairs was performed by standard methods following PCR amplification using specific primers. Sequences of the three independent sets of primers used for sequencing KCNJ5 mutations are as follows:

Set 1 forward primer: KCNJ5-Fn2 (5'-CGACCAAGAGTGGATTCCTT-3')

Set 1 reverse primer: KCNJ5-Rn2 (5'-AGGGTCTCCGCTCTCTTCTT-3')

Set 2 forward primer: KCNJ5-6-F (5'-GCTTCATTTGGTGGCTCATT-3')

Set 2 reverse primer: KCNJ5-6-R (5'-CCACCATGAAGGCATTGAC-3')

Set 3 forward primer: KCNJ5-7-F (5'-GTGTCCGCTTTCCTGTTCTC-3')

Set 3 reverse primer: KCNJ5-7-R (5'-GAGATGACTGCGTTGTTGGA-3')

cDNA synthesis and sequencing. Total RNA was prepared from cryosections using TRIzol reagent (Invitrogen), according to the manufacturer's instructions. DNA-free RNA was prepared using DNAse I (#D5319, Sigma-Aldrich Co). Reverse transcription of 1µg RNA was performed with random hexamer primers using the First-Strand cDNA Synthesis kit (GE Healthcare) according to the manufacturer's instructions. *KCNJ5* cDNA was amplified using intron-spanning primers J5qPCR_F (5'-GGTGACCTGGACCATGTTGGCG-3') and J5qPCR_R (5'-CTTGGCAGGTCATGCCTGTGGC-3') and sequenced with J5cDNA_F (5'-CGACCAAGAGTGGATTCCTT-3') and J5cDNA_R (5'-AGGGTCTCCGCTCTCTTCTT-3') primers.

Structural modeling. Based on a multiple sequence alignment of all known K^+ channel structures, chicken KCNJ12 was used as a model for the KCNJ5 mutations (*S6*). The homotetramer of KCNJ12 was generated from a subunit of KCNJ12 (PDB ID: 3JYC) by applying crystallographic symmetry (I4) using PyMOL software (*S7*). The stereochemistry of the mutated side chains in KCNJ5 were determined with COOT software (*S8*). Hydrogen bonds were identified using PyMOL consistent with the geometry criteria of DSSP (*S9*).

KCNJ5 Immunohistochemistry. Protein expression was analyzed by IHC as described previously (*S10*). In brief, sections (6 µm) from formalin fixed paraffin embedded normal adrenal cortex obtained at adrenalectomy for pheochromocytoma were deparaffinized and subjected to antigen retrieval in 10 mM sodium citrate (pH 6.0) for 15 minutes and were incubated with polyclonal anti-KCNJ5 (#HPA017353, Sigma; 1:100 dilution) and anti-Dab2 (#sc-13982, Santa Cruz; 1:100 dilution). Horseradish peroxidase-conjugated anti-rabbit

secondary antibody was used for visualization of the signal. Sections were counterstained with hematoxylin-eosin.

Molecular Cloning. Human *KCNJ5* was obtained from Origene (#SC119590). The full-length cDNA was sequenced and subcloned into the pIRES2-eGFP vector (Clontech) with EcoRI and BamHI using a PCR-based strategy. Site-directed mutagenesis (Quikchange, Stratagene) was performed to introduce the G151R, T158A, and L168R mutations using the following primers:

J5G151R_F: 5'-CCGAAACAACCATTAGGTATGGCTTCCGAG-3'

J5G151R_R: 5'-CTCGGAAGCCATACCTAATGGTTGTTTCGG-3'

J5T158A_F: 5'-CTTCCGAGTCATCGCAGAGAAGTGTCC-3'

J5T158A_R: 5'-GGACACTTCTCTGCGATGACTCGGAAG-3'

J5L168R_F: 5'-GGATTATACTCCGCTTGGTCCAGGCC-3'

J5L168R_R: 5'-GGCCTGGACCAAGCGGAGTATAATCC-3'.

All mutations were confirmed by sequencing.

cDNA clones encoding human KCNJ3 (Origene #SC118769) and human dopamine receptor D2 (Open Biosystems #MHS1011-74442) were subcloned into the pcDNA3.1(+) vector (Invitrogen) with KpnI and XhoI using PCR-based strategies.

Electrophysiology. 293T cells were transfected with plasmid DNA using TransIT®-293 Transfection Reagent (Mirus) according to the manufacturer's intructions. Empty vector was used as a control. Cells were examined one day after transient transfection. Standard perforated whole-cell patch clamp recordings were performed on GFP-positive cells using an Axopatch

200A (Axon Instruments) amplifier. Pipettes were pulled from borosilicate glass and had resistances between 2 MΩ and 4 MΩ with 140 mM KCl in the pipette.

Electrophysiology of KCNJ3/KCNJ5 heterotetramers. Cells were cotransfected with 0.8 μg wild-type or mutant KCNJ5 and 0.5 μg KCNJ3 cDNA. The extracellular solution contained 140 mM NaCl, 5 mM KCl, 1.8 mM $MgCl_2$, 1.8 mM $CaCl_2$, and 10 mM HEPES (pH 7.4), while the intracellular solution contained 140 mM KCl, 4 mM $MgCl_2$, 1 mM $CaCl_2$, 1 mM EGTA, and 5 mM HEPES (pH 7.4). 1mM $BaCl_2$ was used to block Kir channels. For ion substitution, 140 mM NaCl was replaced with 140 mM choline chloride with or without the presence of $BaCl_2$. The pipette holding potential was 0 mV before clamping, and the cell was clamped from -100 to 60 mV with 20 mV increments. Endogenous currents of 293T cells transfected with empty vector were measured from -100 to 60 mV. These were considered background currents and subtracted from the whole-cell current for each experiment. Data were analyzed by a combination of Axon Clampfit9.2 (Molecular Devices) and SigmaPlot (Jandel Scientific) programs. Data from 3-7 cells were analyzed for each construct. All data are shown as mean ± SEM. Cell capacitances varied between 24.5 and 26 pF, and were used to normalize currents to that of a 25 pF cell.

The relative permeability of K^+ to Na^+ was estimated from the reversal potential using the Goldman equation with K^+ and Na^+ as the predominant permeant cations, consistent with experimental data.

$$E_{rev} = \frac{RT}{F} \cdot ln \frac{p_K [K^+]_o + p_{Na} [Na^+]_o}{p_K [K^+]_i + p_{Na} [Na^+]_i}$$

E_{rev}, reversal potential; p, permeability; R, gas constant; T, temperature (24°C); F, Faraday's constant.

For measurement of KCNJ3/KCNJ5 response to GPCR activation, 0.5 μg type 2 dopamine receptor (D2R) cDNA was added to the transfection, and cells were stimulated by addition of 1 μM dopamine hydrochloride (Sigma) to the extracellular solution prior to current measurements.

Electrophysiology of KCNJ5 homotetramers. To analyze homomeric wild-type or mutant KCNJ5 currents, 1 μg of cDNA was transfected. Because KCNJ5 homotetramers have a low current, symmetrical high Na^+ and high K^+ solutions were separately used to increase the current (*S11, S12*). For each construct we measured currents in two conditions. In one, the extracellular solution contained 140 mM NaCl, 5 mM KCl, 1.8 mM $MgCl_2$, 1.8 mM $CaCl_2$, and 10 mM HEPES, pH 7.4, and the intracellular solultion was the same except it also had 2 mM EGTA; in the other, the extracellular solution contained 140 mM KCl, 0.5 mM $MgCl_2$, 1.5 mM $CaCl_2$, and 10 mM HEPES, pH 7.4, and the intracellular solution 140 mM KCl, 4 mM $MgCl_2$, 1 mM $CaCl_2$, 1 mM EGTA, and 5 mM HEPES, pH 7.4. Electrophysiology protocol and analysis was as above for KCNJ5/KCNJ3 heterotetramers. For determination of the reversal potential, the extracellular solution contained 140 mM NaCl, 5 mM KCl, 1.8 mM $MgCl_2$, 1.8 mM $CaCl_2$, and 10 mM HEPES (pH 7.4), while the intracellular solution contained 140 mM KCl, 4 mM $MgCl_2$, 1 mM $CaCl_2$, 1 mM EGTA, and 5 mM HEPES (pH 7.4). 1 mM $BaCl_2$ was added to test sensitivity of currents to barium. The reversal potential was determined using a ramp protocol ranging from -100 to +100 mV after forming a high resistance seal. The test was repeated at least twice in each cell, and 3 cells were studied for each construct.

Western blotting. 293T cells transfected with WT or mutant KCNJ5 plus KCNJ3 as above were harvested and lysed in a buffer containing 50 mM HEPES pH 7.4, 250 mM NaCl, 1.5 mM $MgCl_2$, 1mM EGTA pH 8.0, 10% glycerol, 1% Triton X-100 and protease inhibitors (Roche). Cleared lysates were quantified by a BCA assay (Pierce); equal amounts were fractionated by SDS-PAGE and transferred to a PVDF membrane (Millipore). The membrane was blocked and incubated with anti-KCNJ5 (Sigma, #HPA017353, 1:500 dilution), followed by a HRP-conjugated secondary antibody. Bands were visualized by ECL (GE Healthcare). The blot was incubated in ECL stripping buffer at 65°C for 45 min, re-blocked, and incubated with an anti-KCNJ3 antibody (Alomone #APC-005, 1:1000 dilution), again followed by a HRP-conjugated secondary antibody.

Orthologs and paralogs. Full-length orthologous protein sequences were identified by a BLAST search of human KCNJ5 and extracted from GenBank. Orthologs were confirmed based on database identity of annotation or in a BLAST of the protein sequence against the human protein sequence, with the requirement that human KCNJ5 be the top hit. Protein sequences were aligned using the ClustalW algorithm. GenBank accession numbers were: NP_000881.3 (human), NP_034735.3 (mouse), XP_417864.2 (chicken), NP_001016901.1 (frog), XP_700619.4 (zebrafish), and XP_002122831.1 (tunicate). For human inward rectifier paralogs, GenBank accession numbers were: NP_000211.1 (KCNJ1), NP_000882.1 (KCNJ2), NP_066292.2 (KCNJ12), NP_002230.1 (KCNJ3), NP_002232.2 (KCNJ10), NP_733938.1 (KCNJ16), NP_004973.1 (KCNJ8), and NP_002233.2 (KCNJ13).

Adrenal Cortical Gene Expression. Normal human adrenal cortical tissue from two patients undergoing adrenalectomy for pheochromocytoma at University Hospital, Uppsala was dissected and determined by histology to be free of tumor or adrenal medulla tissue. Tissue processing and hybridization were performed in duplicate using the Human Gene 1.0 ST Array (Affymetrix). Raw intensity data from the 4 hybridizations was normalized by RMA method implemented in R package *affy* (*S13*).

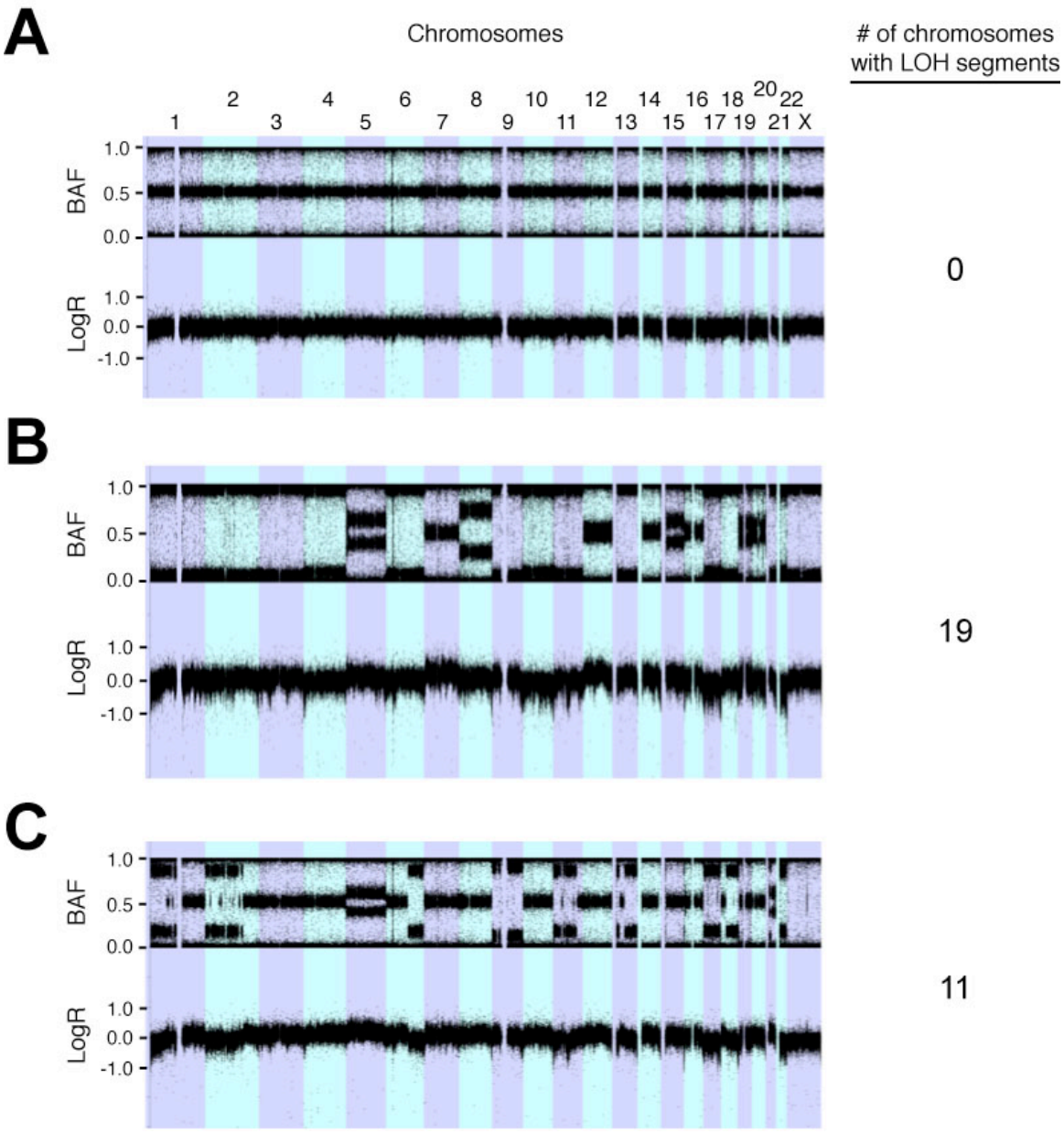

Fig. S1. Loss of heterozygosity (LOH) in aldosterone-producing adenomas. Genome-wide distribution of intensity (LogR) and B-allele fraction (BAF) from APA tumors with varying degree of LOH. The number of LOH-affected chromosomes is shown on the right. (A) Plot of tumor APA12 without any LOH. (B, C) Plots of tumors with LOH (APA21 and APA5, respectively).

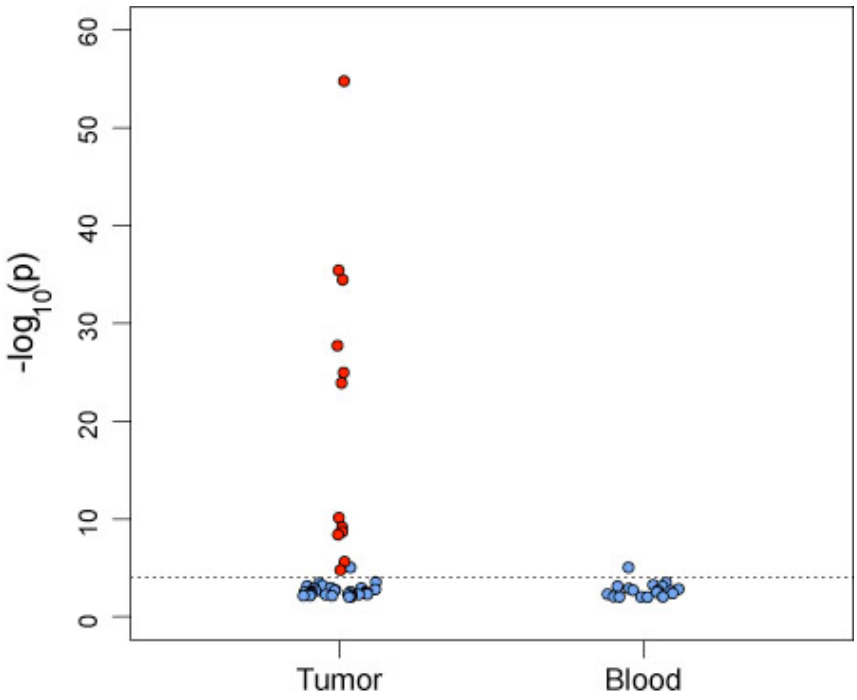

Fig. S2. p-value distribution of putative somatic mutations in APAs. $-\log_{10}$ p-values from Fisher's exact test for the significance of read count differences of putative somatic mutations in tumor samples (Tumor) using blood as a reference; as control, the p-value distribution of variants in blood (labeled Blood) seen in excess using tumor reads as a reference. Analysis further described in Methods. Mutations validated by Sanger sequencing are shown as red symbols. Dotted line denotes $p = 10^{-4}$.

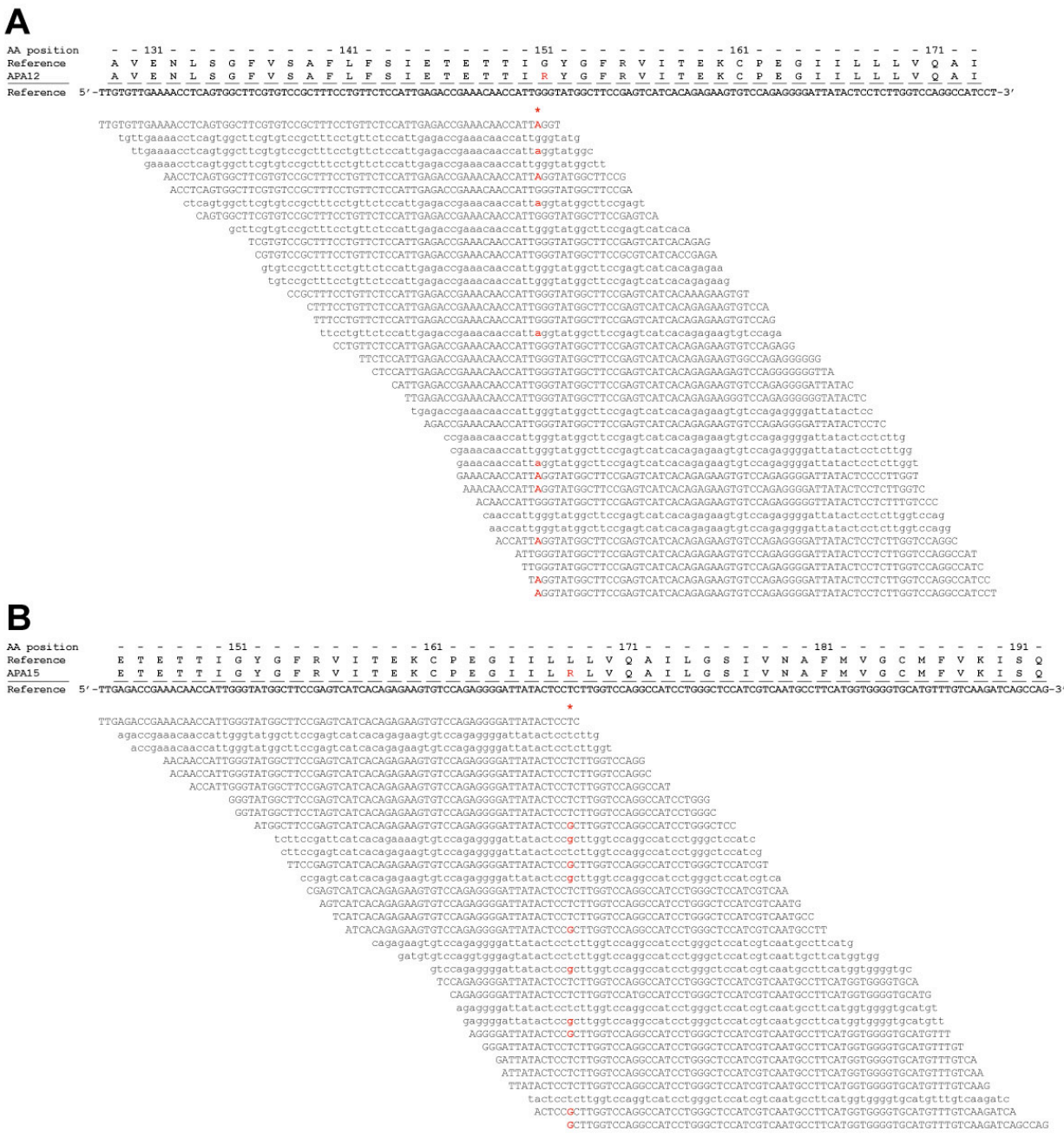
A
AA position - - 131 - - - - - - - - - - 141 - - - - - - - - - - 151 - - - - - - - - - - 161 - - - - - - - - - - 171 - -
Reference A V E N L S G F V S A F L F S I E T E T T I G Y G F R V I T E K C P E G I I L L L V Q A I
APA12 A V E N L S G F V S A F L F S I E T E T T I R Y G F R V I T E K C P E G I I L L L V Q A I
Reference 5′-TTGTGTTGAAAACCTCAGTGGCTTCGTGTCCGCTTTCCTGTTCTCCATTGAGACCGAAACAACCATTGGGTATGGCTTCCGAGTCATCACAGAGAAGTGTCCAGAGGGGATTATACTCCTCTTGGTCCAGGCCATCCT-3′
B
AA position - - - - - - 151 - - - - - - - - - - 161 - - - - - - - - - - 171 - - - - - - - - - - 181 - - - - - - - - - - 191 -
Reference E T E T T I G Y G F R V I T E K C P E G I I L L L V Q A I L G S I V N A F M V G C M F V K I S Q
APA15 E T E T T I G Y G F R V I T E K C P E G I I L R L V Q A I L G S I V N A F M V G C M F V K I S Q
Reference 5′-TTGAGACCGAAACAACCATTGGGTATGGCTTCCGAGTCATCACAGAGAAGTGTCCAGAGGGGATTATACTCCTCTTGGTCCAGGCCATCCTGGGCTCCATCGTCAATGCCTTCATGGTGGGGTGCATGTTTGTCAAGATCAGCCAG-3′

Fig. S3. Mutations in *KCNJ5* in aldosterone-producing adenomas in Illumina sequence reads. Selected independent reads that cover the mutated positions are shown. At the top of each panel, reference amino acid and DNA sequences are shown with independent Illumina reads shown below with forward (capital) and reverse (lower cases) orientations. Base calls showing somatic mutations are highlighted in red. (A) G151R mutation from APA12. (B) L168R mutation from APA15. Complete set of independent reads at these positions indicated in Table 1.

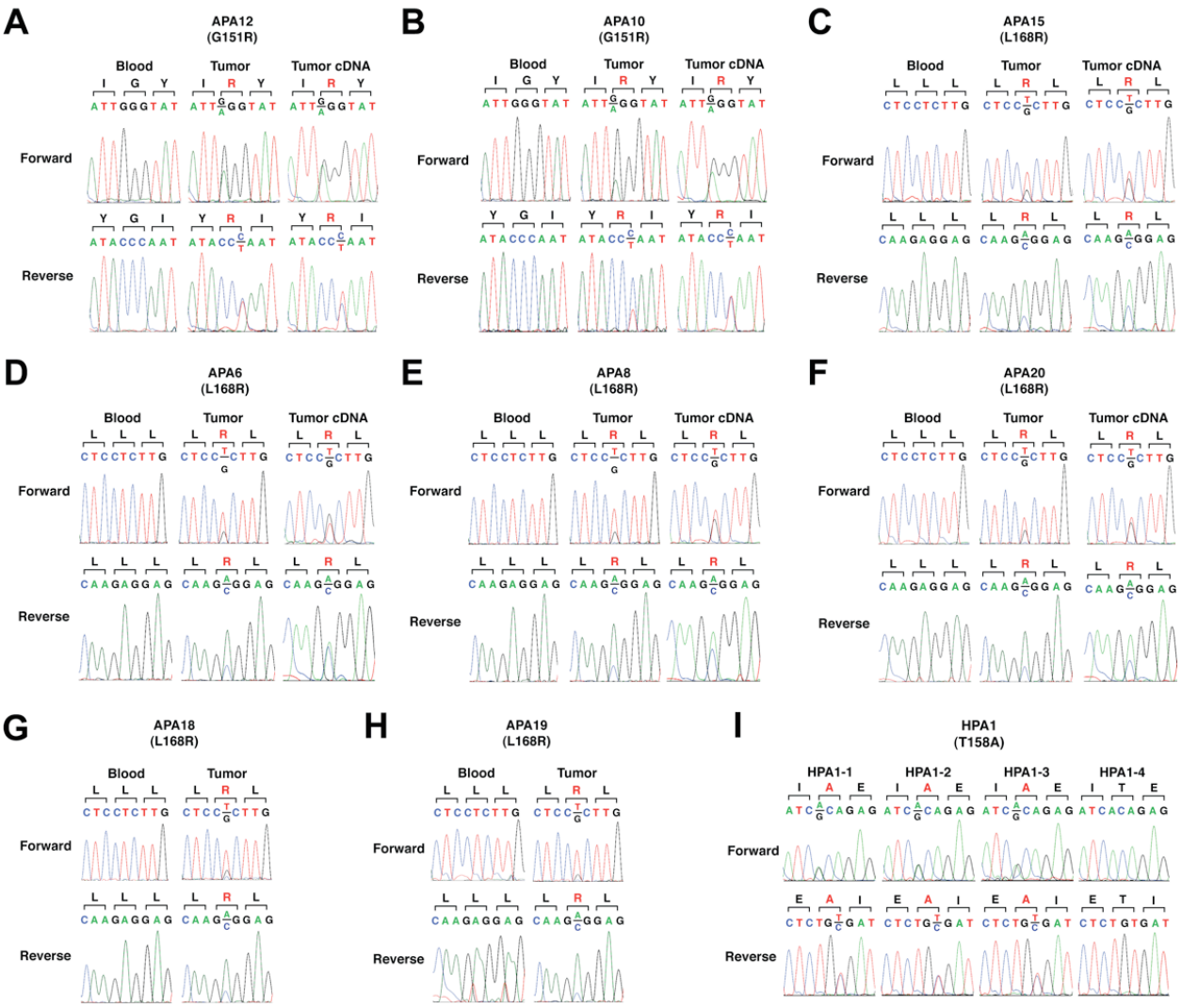

Fig. S4. Mutations in *KCNJ5* in aldosterone-producing adenoma and inherited primary aldosteronism. Sanger traces from 8 tumor samples with somatic mutations G151R or L168R in *KCNJ5* (A-H) along with confirmation sequences from tissue cDNA (A-F) are shown. (I) Sanger traces of T158A mutation from kindred HPA1. Kindred ID's as in Fig. 1C.

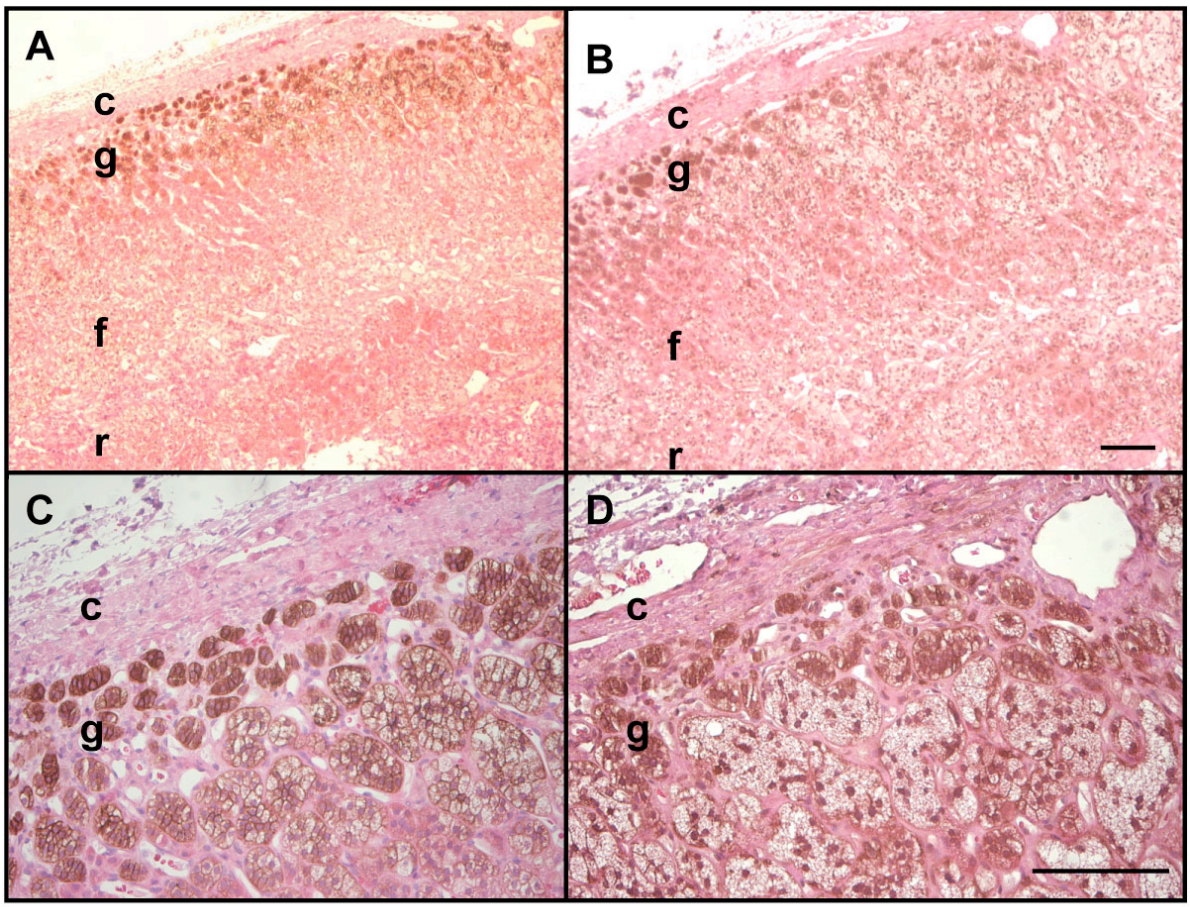

Fig. S5. KCNJ5 expression in adrenal glomerulosa. Human adrenal cortex was stained with anti-KCNJ5 (A,C) or anti-Dab2 (an adrenal glomerulosa marker; B,D) using horseradish peroxidase-conjugated anti-rabbit secondary antibody, and sections were counterstained with hematoxylin-eosin. Low-power (A,B) and high power views (C,D) demonstrate staining of the glomerulosa cells in the outermost cell layers of the adrenal cortex with both anti-KCNJ5 and anti-Dab2 antibodies. 'c' denotes adrenal capsule; 'g', glomerulosa; 'f', fasciculata; 'r', reticularis. Scale bars: 100 μm.

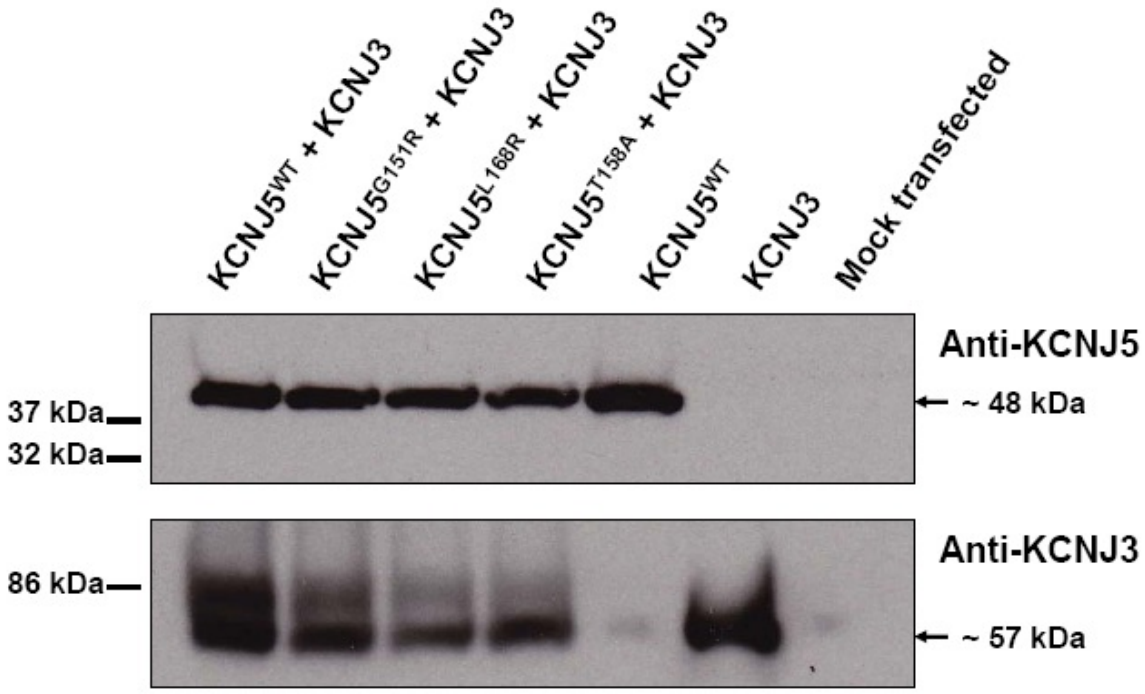

Fig. S6. KCNJ5 expression in transiently transfected 293T cells. Lysates of 293T cells transfected with WT or mutant KCNJ5 and/or KCNJ3, or mock-transfected cells, were denatured, fractionated by SDS-PAGE, transferred to membranes and incubated with antibodies to KCNJ5 (top) or anti-KCNJ3 (bottom) as described in Methods. Monomeric KCNJ5 is detected as a single band at the calculated molecular weight of ~48 kDa, while monomeric KCNJ3 shows 2 species- one of ~57 kDa and a second, presumably glycosylated version that migrates with an apparent molecular weight of 86 kDa (*S14*).

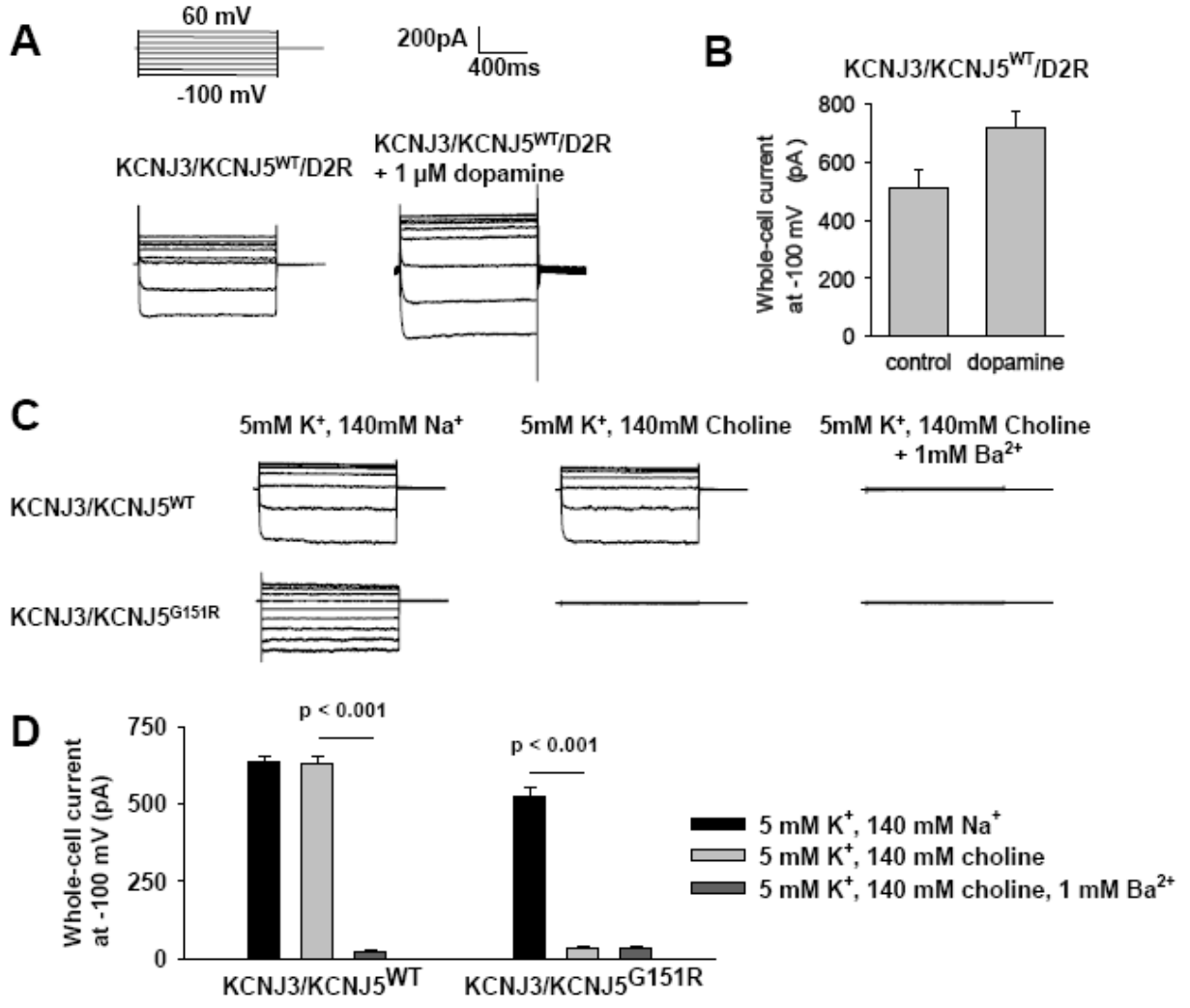

Fig. S7. Effect of dopamine and choline substitution on current in 293T cells. (A) Increased KCNJ3/KCNJ5 channel activity stimulated by dopamine. KCNJ3/KCNJ5 heterotetramers are known to show increased activity in response to dopamine. Representative whole-cell recordings of 293T cells cotransfected with KCNJ3/KCNJ5^{WT} and the dopamine D2 receptor are shown. The pipette holding potential was 0 mV before clamping, and the cell was clamped from -100 to 60 mV with 20 mV increments before (left) and after (right) addition of 1µM dopamine as described in Methods. The extracellular solution contained 140 mM NaCl, 5 mM KCl, 1.8 mM

$MgCl_2$, 1.8 mM $CaCl_2$, and 10 mM HEPES, pH 7.4, while the intracellular solution contained 140 mM KCl, 4 mM $MgCl_2$, 1 mM $CaCl_2$, 1 mM EGTA, and 5 mM HEPES, pH 7.4. Dopamine is seen to increase current. (B) Mean ± SEM of current amplitudes measured at -100mV before (control) and after addition of dopamine as in panel A (n = 4). Dopamine increases current by ~50%, consistent with prior observations on KCNJ3/KCNJ5 heterotetramers. (C) Elimination of extracellular Na^+ inhibits KCNJ3/KCNJ5^{G151R} but not KCNJ3/KCNJ5^{WT}. In Fig. 3, Na^+ was eliminated from the extracellular fluid by substitution for choline in the presence of Ba^{2+}. Because Ba^{2+} inhibits the WT channel, we could not assess in this experiment whether elimination of Na^+ alone had effects on the WT channel. We were also interested in whether KCNJ3/KCNJ5^{G151R} channels were inhibited by elimination of Na^+ in the absence of Ba^{2+}. Representative whole-cell recordings of 293T cells transfected with KCNJ3/KCNJ5^{WT} or KCNJ3/KCNJ5^{G151R} are shown. Left column: The extracellular solution contained 140 mM NaCl, 5 mM KCl, 1.8 mM $MgCl_2$, 1.8 mM $CaCl_2$, and 10 mM HEPES, while the intracellular solution contained 140 mM KCl, 4 mM $MgCl_2$, 1 mM $CaCl_2$, 1 mM EGTA, and 5 mM HEPES. Middle column: 140 mM choline chloride is substituted for extracellular NaCl. Right column: 1mM $BaCl_2$ was added. (D) Mean ± SEM of current amplitudes at -100 mV from 3 cells in each condition described in (C). Elimination of extracellular Na^+ has no effect on KCNJ3/KCNJ5^{WT} but markedly inhibits currents in cells expressing KCNJ3/KCNJ5^{G151R} ($p < 0.001$, Student's t-test).

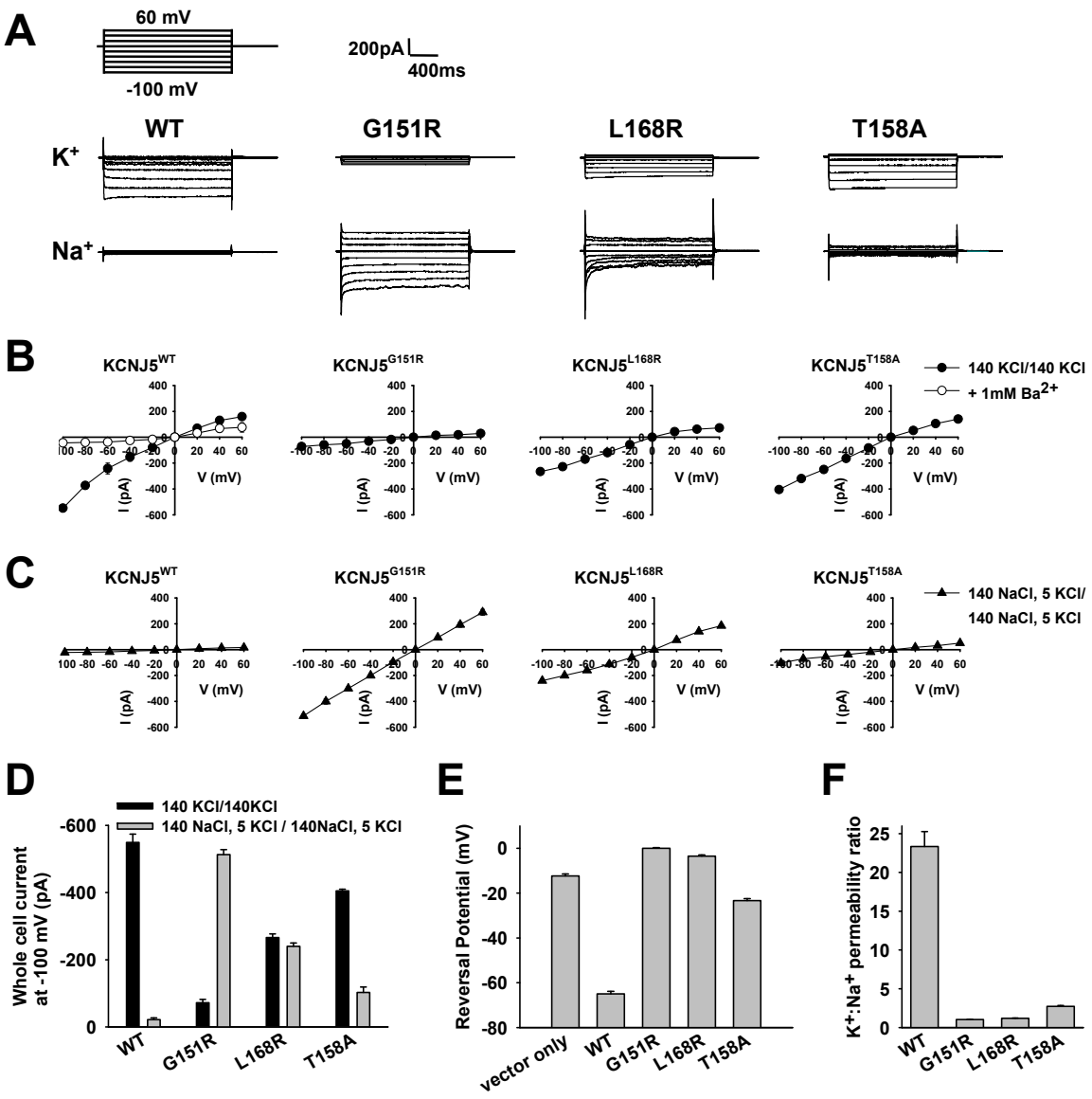

Fig. S8. Mutations in KCNJ5 homotetramers increase Na^+ conductance. Because of low current amplitude of homotetrameric channels, currents were measured under symmetrical high Na^+ or high K^+ conditions, which increases current amplitude (*S11, S12*) (A-D); reversal potentials and permeability ratios were determined using physiological solutions (E, F). (A) Representative whole-cell recordings showing K^+ and Na^+ currents in 293T cells transfected with KCNJ5, $KCNJ5^{G151R}$, $KCNJ5^{L168R}$, and $KCNJ5^{T158A}$. The extracellular solution for Na^+ current

measurements contained 140 mM NaCl, 5 mM KCl, 1.8 mM $MgCl_2$, 1.8 mM $CaCl_2$, and 10 mM HEPES, pH=7.4 and the intracellular solution (pipette) was identical to the extracellular solution except for the addition of 2 mM EGTA; for K^+ current measurements, the extracellular solution contained 140 mM KCl, 0.5 mM $MgCl_2$, 1.5 mM $CaCl_2$, and 10 mM HEPES, pH 7.4 and the intracellular solution 140 mM KCl, 4 mM $MgCl_2$, 1 mM $CaCl_2$, 1 mM EGTA, and 5 mM HEPES, pH 7.4. The pipette holding potential was 0 mV before clamping, and the cell was clamped from -100 to 60 mV with 20 mV increments. (B, C) Current-voltage relationships from cells expressing the indicated constructs with symmetric high K^+ or high Na^+ solutions as in (A). Addition of 1 mM $BaCl_2$ to the extracellular fluid in panel (B) inhibited WT channel activity. (D) K^+ (black) and Na^+ (gray) mean current amplitudes determined at -100 mV from cells expressing WT and mutant KCNJ5 as in (A, B), demonstrating increased Na^+, and decreased K^+ conductance in the mutant channels ($n \geq 3$ for each condition). Relative permeabilities of K^+:Na^+ were determined in physiologic solutions as described in panel (E). (E) Reversal potential of 293T cells transfected with WT or mutant KCNJ5 using physiological solutions. The extracellular solution contained 140 mM NaCl, 5 mM KCl, 1.8 mM $MgCl_2$, 1.8 mM $CaCl_2$, and 10 mM HEPES (pH 7.4), while the intracellular solution contained 140 mM KCl, 4 mM $MgCl_2$, 1 mM $CaCl_2$, 1 mM EGTA, and 5 mM HEPES (pH 7.4). The reversal potential for the homotetramers was determined by a ramp protocol ranging from -100 to +100 mV after forming a high resistance seal. The test was repeated at least twice in the same cell, and 3 cells were studied for each construct. (F) The K^+:Na^+ permeability ratio for homotetrameric WT and mutant channels was estimated from the Goldman equation: WT = 23.3 ± 1.9:1; G151R = 1.0 ± 0.1:1; L168R = 1.2 ± 0.1:1; T158A = 2.7 ± 0.1:1. These values are very similar to values from KCNJ3/KCNJ5 heterotetramers. Data in (B) – (F) are shown as mean ± SEM. Reversal

potentials and K^+:Na^+ permeability ratios are significantly different between wild-type and mutant channels (all p <0.001 by Student's t-test).

Table S1. Clinical features of 22 patients with aldosterone-producing adenomas.

Patient	Age	Gender	ARR	Tumor Weight (g)	Tumor Diameter (mm)	HTN	Serum K^+ (mmol/L)	# of LOH chromosomes	Tumor KCNJ5 genotype
APA10	57	F	438	12	23	+	3.8	0	G151R/+
APA12	34	F	1,250	15.2	25	+	3.7	0	G151R/+
APA6	48	F	332	11	8	+	3.4	0	L168R/+
APA8	33	F	718	9.3	20	+	3.9	0	L168R/+
APA15	34	M	700	14	25	+	3.1	0	L168R/+
APA19	56	F	230	NA	20	+	3.4	0	L168R/+
APA20	31	F	457	NA	22	+	2.5^	0	L168R/+
APA18	37	F	480	13.8	40	+	4.5	1	L168R/+
APA16	34	F	259	NA	46	+	3.4	0	WT
APA9	28	F	256	46	48	+	3.4	0	WT
APA11	39	M	500	9.7	10	+	2.9^	0	WT
APA22	65	F	271	NA	25	+	3.9	0	WT
APA1	44	F	235*	8.5	9	+	3.3	1	WT
APA4	59	F	284	35	41	+	3.6	4	WT
APA5	62	M	241	22	24	+	4.1	11	WT
APA14	60	M	246	NA	45	+	3.8	11	WT
APA7	53	F	482	41	45	+	3.5	13	WT
APA2	34	M	356*	21	25	+	3.4	15	WT
APA3	63	F	618	14	20	+	2.8^	16	WT
APA17	59	M	243	NA	32	+	3.8	17	WT
APA13	53	F	317	31	38	+	3.5	19	WT
APA21	57	F	326	28	32	+	3.5	19	WT
Mean	47.3	NA	420.0	20.7	28.3	NA	3.5	5.8	NA
SD	12.5	NA	239.0	12.0	12.2	NA	0.4	7.5	NA

ARR: aldosterone:renin ratio in (pmol/L)/(mIU/L plasma renin concentration) (> 50 indicative of primary aldosteronism) except two subjects (*) in whom ARR was measured in (pmol/L)/(mg/L/h plasma renin activity) (> 100 indicative of primary aldosteronism); HTN: hypertension; Serum K^+: preoperative serum potassium (reference range 3.5-5.0 mmol/l) while on potassium therapy except in three subjects, without potassium supplementation (^); # of LOH chromosomes: number of chromosomes with loss of heterozygosity; NA, not available.

Table S2. Summary sequence statistics of tumor-blood pairs.

Sample	**APA9**		**APA12**		**APA15**		**APA22**	
Source	Blood	Tumor	Blood	Tumor	Blood	Tumor	Blood	Tumor
# of total bases	16.9 Gb	17.3 Gb	16.9 Gb	16.7 Gb	15.8 Gb	15.2 Gb	17.1 Gb	16.3 Gb
% of bases mapping to genome	97.6%	98.4%	96.3%	95.7%	98.1%	99.2%	98.2%	98.5%
% of bases mapping to exome	62.7%	63.2%	61.9%	47.2%	63.8%	69.2%	64.4%	64.9%
Mean unique reads per targeted base	178.8X	165.3X	190.4X	156.8X	152.9X	118.6X	210.0X	193.0X
% of bases read at least 8x	96.5%	96.5%	96.7%	96.6%	94.3%	96.5%	96.7%	97.2%
Sensitivity of heterozygote detection	98.6%	98.6%	98.8%	98.8%	95.9%	98.4%	99.0%	98.8%
Specificity of heterozygous calls	99.9%	99.9%	99.9%	99.9%	99.8%	99.8%	99.9%	99.9%

Gb, 10^9 bases; Sensitivity, % of heterozygous calls by SNP genotyping that were called heterozygous by sequencing; Specificity, % of heterozygous calls by sequence at genotyped SNP positions called heterozygous by SNP genotyping.

Table S3. Potential somatic mutations in APAs.

Patient	Chr	Position	Validated by Sanger sequence	Base change	Gene	Effect on protein	# of reads from tumor			# of reads from blood		p-value
							Ref. allele	Non-ref. allele	% of all reads	Ref. allele	Non-ref. allele	
APA9	14	99,813,560	Yes	C>G	*YY1*	T372R	115	69	37.5%	184	0	1.3×10^{-24}
	9	114,858,771	Yes	C>G	*ZFP37*	V7L	47	23	32.9%	77	0	4.0×10^{-9}
	2	29,301,916	No	T>G	*ALK*	P1029P	58	14	19.4%	84	0	9.4×10^{-6}
	10	79,240,978	No	C>A	*DLG5*	G1448V	61	9	12.9%	97	0	2.9×10^{-4}
	12	54,844,521	No	T>G	*SMARCC2*	N1134T	41	9	18.0%	65	0	2.2×10^{-3}
	11	107,886,725	No	G>T	*EXPH5*	N1497K	148	18	10.8%	93	1	2.4×10^{-3}
	10	91,493,640	No	A>G	*KIF20B*	K1297K	15	18	54.5%	10	0	2.4×10^{-3}
	19	43,347,213	No	C>G	*SIPA1L3*	G1345G	32	6	15.8%	75	1	5.4×10^{-3}
	4	15,052,910	No	C>A	*C1QTNF7*	P87T	66	11	14.3%	49	0	6.6×10^{-3}
	5	153,170,839	No	G>C	*GRIA1*	R861P	32	9	22.0%	41	1	7.1×10^{-3}
	1	20,347,475	No	T>C	*PLA2G2F*	P210P	81	10	11.0%	89	1	9.5×10^{-3}
	12	51,195,227	No	A>C	*KRT5*	G513G	42	5	10.6%	69	0	9.6×10^{-3}
APA12	11	86,341,084	Yes	C>A	*FZD4*	C121F	491	139	22.1%	871	0	1.6×10^{-55}
	11	**128,286,829**	**Yes**	**G>A**	***KCNJ5***	**G151R**	**120**	**59**	**33.0%**	**290**	**0**	$\mathbf{1.9 \times 10^{-28}}$
	12	56,159,261	Yes	G>A	*ARHGAP9*	R66C	149	65	30.4%	282	1	1.1×10^{-25}
	1	7,783,809	No	A>C	*PER3*	P280P	35	11	23.9%	40	0	6.4×10^{-4}
	12	75,302,194	No	C>A	*OSBPL8*	G492V	62	8	11.4%	82	0	1.6×10^{-3}
	11	64,654,840	No	T>G	*SYVN1*	T325P	19	5	20.8%	55	0	1.9×10^{-3}
	9	12,765,880	No	T>G	*C9orf150*	C56G	13	10	43.5%	19	1	5.0×10^{-3}
APA15	5	7,573,931	Yes	C>G	*ADCY2*	V163V	154	65	29.7%	466	0	3.7×10^{-36}
	11	**128,286,881**	**Yes**	**T>G**	***KCNJ5***	**L168R**	**159**	**65**	**29.0%**	**456**	**0**	$\mathbf{3.5 \times 10^{-35}}$
	X	53,239,430	Yes	C>T	*KDM5C*	V1341M	30	30	50.0%	54	0	7.6×10^{-11}
	7	30,662,070	Yes	G>A	*CRHR2*	Y305Y	103	28	21.4%	123	0	2.1×10^{-9}
	4	9,498,340	Yes	G>A	*SLC2A9*	L414L	45	18	28.6%	58	0	2.4×10^{-6}
	13	18,965,011	No	A>C	*TPTE2*	L33R	90	11	10.9%	98	0	7.4×10^{-4}
	7	100,465,288	No	A>T	*MUC17*	T1291S	67	11	14.1%	63	0	1.1×10^{-3}
	14	64,058,677	No	T>C	*ZBTB1*	H234H	14	14	50.0%	17	1	2.9×10^{-3}
	7	100,465,280	No	C>A	*MUC17*	T1288K	59	9	13.2%	63	0	3.1×10^{-3}
	3	99,466,292	No	T>C	*OR5H6*	I158I	137	25	15.4%	56	1	3.8×10^{-3}
	11	36,570,975	No	T>G	*RAG2*	K440N	52	7	11.9%	96	1	4.9×10^{-3}
	7	100,465,247	No	G>T	*MUC17*	S1277I	68	9	11.7%	59	0	5.2×10^{-3}
	11	125,376,945	No	C>T	*CDON*	A679A	32	16	33.3%	22	1	7.3×10^{-3}
APA22	21	43,054,087	Yes	G>A	*PDE9A*	Exon 13 splice donor GT>AT	90	31	25.6%	123	0	6.8×10^{-10}
	2	140,918,376	Yes	T>G	*LRP1B*	R3429S	60	14	18.9%	80	0	1.7×10^{-5}
	12	75,296,439	No	T>A	*OSBPL8*	L551F	66	10	13.2%	86	0	3.7×10^{-4}
	17	7,520,431	No	G>C	*TP53*	N30K	58	9	13.4%	66	0	2.9×10^{-3}
	17	7,520,430	No	C>T	*TP53*	V31I	62	9	12.7%	68	0	3.0×10^{-3}
	17	4,581,880	No	C>G	*MED11*	A49G	21	8	27.6%	38	1	3.6×10^{-3}
	12	111,376,841	No	T>C	*PTPN11*	L206L	88	10	10.2%	106	1	3.7×10^{-3}
	12	52,682,649	No	T>G	*HOXC9*	V236G	80	11	12.1%	90	1	4.9×10^{-3}
	5	43,648,945	No	T>G	*NNT*	G110G	49	12	19.7%	49	1	5.7×10^{-3}

Table S4. Expression of K^+ channels in human adrenal cortex.

Gene ID	Gene	Expression	Gene ID	Gene	Expression	Gene ID	Gene	Expression
NM_000218	*KCNQ1*	10.45	NM_020822	*KCNT1*	7.12	NM_139136	*KCNC2*	6.29
NM_001017425	*KCNK2*	10.36	NM_002249	*KCNN3*	7.11	NM_002243	*KCNJ15*	6.17
NM_002246	*KCNK3*	10.32	NM_012282	*KCNE1L*	7.11	NM_004974	*KCNA2*	6.11
NM_000890	*KCNJ5*	9.85	NM_000219	*KCNE1*	7.05	NM_002245	*KCNK1*	6.11
NM_014505	*KCNMB4*	9.38	NM_014591	*KCNIP2*	7.04	NM_002252	*KCNS3*	6.07
NM_002233	*KCNA4*	8.71	NM_152868	*KCNJ4*	6.96	NM_004700	*KCNQ4*	6.05
NM_004982	*KCNJ8*	8.37	NM_000891	*KCNJ2*	6.96	NM_170720	*KCNJ14*	6.05
NM_021614	*KCNN2*	8.21	NM_002250	*KCNN4*	6.93	NM_001160133	*KCNQ5*	6.05
NM_004823	*KCNK6*	8.05	NM_172347	*KCNG4*	6.92	NM_172362	*KCNH1*	6.01
NM_001014797	*KCNMA1*	8.03	NM_002237	*KCNG1*	6.89	NM_003471	*KCNAB1*	5.95
NM_022358	*KCNK15*	8.02	NM_020697	*KCNS2*	6.89	NM_181840	*KCNK18*	5.95
NM_003740	*KCNK5*	7.87	NM_001135105	*KCNK16*	6.83	NM_002234	*KCNA5*	5.93
NM_004978	*KCNC4*	7.85	NM_004983	*KCNJ9*	6.82	NM_005472	*KCNE3*	5.90
NM_133329	*KCNG3*	7.77	NM_012285	*KCNH4*	6.77	NM_031886	*KCNA7*	5.90
NM_012283	*KCNG2*	7.76	NM_001034837	*KCNIP1*	6.71	NM_133497	*KCNV2*	5.74
NM_003636	*KCNAB2*	7.73	NM_144633	*KCNH8*	6.70	NM_031460	*KCNK17*	5.72
NR_024627	*KCNQ1DN*	7.68	NM_022054	*KCNK13*	6.68	NM_004732	*KCNAB3*	5.66
NM_080671	*KCNE4*	7.66	NM_004137	*KCNMB1*	6.62	NM_139318	*KCNH5*	5.64
NM_005714	*KCNK7*	7.61	NM_030779	*KCNH6*	6.56	NM_021161	*KCNK10*	5.63
NM_004976	*KCNC1*	7.50	NM_000217	*KCNA1*	6.54	NM_002232	*KCNA3*	5.61
NM_022055	*KCNK12*	7.37	NM_000525	*KCNJ11*	6.53	NM_002251	*KCNS1*	5.45
NM_004519	*KCNQ3*	7.37	NM_172107	*KCNQ2*	6.50	NM_147182	*KCNIP4*	5.38
NM_021012	*KCNJ12*	7.34	NM_002237	*KCNG1*	6.49	NM_012281	*KCND2*	5.31
NM_016601	*KCNK9*	7.33	NM_004979	*KCND1*	6.44	NM_170742	*KCNJ16*	5.23
NM_013434	*KCNIP3*	7.33	NM_198503	*KCNT2*	6.42	NM_005832	*KCNMB2*	5.22
NM_005549	*KCNA10*	7.27	NM_004770	*KCNB2*	6.42	NM_002241	*KCNJ10*	5.11
NM_000238	*KCNH2*	7.24	NM_002248	*KCNN1*	6.38	NM_171830	*KCNMB3*	5.08
NM_004977	*KCNC3*	7.20	NM_014379	*KCNV1*	6.35	NM_033272	*KCNH7*	4.93
NM_012284	*KCNH3*	7.17	NM_002235	*KCNA6*	6.34	NM_172201	*KCNE2*	4.92
NM_033310	*KCNK4*	7.15	NM_004975	*KCNB1*	6.34	NM_002240	*KCNJ6*	4.85
NM_002236	*KCNF1*	7.15	NM_004980	*KCND3*	6.30	NM_002242	*KCNJ13*	4.82
NM_173605	*KCNRG*	7.14	NM_002239	*KCNJ3*	6.30	NM_153767	*KCNJ1*	4.67
(Continued)			(Continued)			S56770	*KCNC1*	3.91

Expression of potassium channels in human adrenal cortex. Expression shown in $\log_2$ scale.

Mean expression of all genes is 7.196.

Table S5. Clinical presentation of affected individuals in kindred HPA1 (adapted from (*S2*)).

Patient	Age at presentation (years)	Gender	Blood Pressure (mmHg)	PRA (ng/ml/h)	Serum Aldosterone (ng/dl)	24-h urine Aldosterone (µg/24h)	Serum K^+ (mmol/l)	*KCNJ5* Genotype
HPA1-1	5	Male	230/140	NA	NA	67	2.8	T158A/+
HPA1-2	7	Female	188/140	0.3	137.4	NA	1.8	T158A/+
HPA1-3	4	Female	148/114	0.2	185.1	NA	1.9	T158A/+

PRA: Plasma renin activity (reference range 0.4-8.8 ng/ml/h); Serum Aldosterone (reference range 3-39.5 ng/dl); 24-h urine aldosterone (reference range 1-8 µg/24h); Serum K^+: serum potassium concentration (reference range 3.5-5 mmol/liter); NA: not available.

Supporting Online Material References:

S1. J. W. Funder*, et al.*, Case detection, diagnosis, and treatment of patients with primary aldosteronism: an endocrine society clinical practice guideline. *J Clin Endocrinol Metab* **93**, 3266-81 (2008).

S2. D. S. Geller*, et al.*, A novel form of human mendelian hypertension featuring nonglucocorticoid-remediable aldosteronism. *J Clin Endocrinol Metab* **93**, 3117-23 (2008).

S3. M. Choi*, et al.*, Genetic diagnosis by whole exome capture and massively parallel DNA sequencing. *Proc Natl Acad Sci U S A* **106**, 19096-101 (2009).

S4. H. Li, J. Ruan, R. Durbin, Mapping short DNA sequencing reads and calling variants using mapping quality scores. *Genome Res* **18**, 1851-8 (2008).

S5. H. Li*, et al.*, The Sequence Alignment/Map format and SAMtools. *Bioinformatics* **25**, 2078-9 (2009).

S6. X. Tao, J. L. Avalos, J. Chen, R. MacKinnon, Crystal structure of the eukaryotic strong inward-rectifier K+ channel Kir2.2 at 3.1 A resolution. *Science* **326**, 1668-74 (2009).

S7. W. L. DeLano, The PyMOL molecular graphics system. *DeLano Scientific, San Carlos, CA, USA*. (2002).

S8. P. Emsley, K. Cowtan, Coot: model-building tools for molecular graphics. *Acta Crystallogr D Biol Crystallogr* **60**, 2126-32 (2004).

S9. W. Kabsch, C. Sander, Dictionary of protein secondary structure: pattern recognition of hydrogen-bonded and geometrical features. *Biopolymers* **22**, 2577-637 (1983).

S10. P. Bjorklund, G. Akerstrom, G. Westin, Accumulation of nonphosphorylated beta-catenin and c-myc in primary and uremic secondary hyperparathyroid tumors. *J Clin Endocrinol Metab* **92**, 338-44 (2007).

S11. J. M. Owen, C. C. Quinn, R. Leach, J. B. Findlay, M. R. Boyett, Effect of extracellular cations on the inward rectifying K+ channels Kir2.1 and Kir3.1/Kir3.4. *Exp Physiol* **84**, 471-88 (1999).

S12. T. Andreoli*, et al.*, Eds., *Molecular Biology of Membrane Transport Disorders* (Plenum Press, New York, ed. 2, 1996), chap. 5.

S13. L. Gautier, L. Cope, B. M. Bolstad, R. A. Irizarry, affy--analysis of Affymetrix GeneChip data at the probe level. *Bioinformatics* **20**, 307-15 (2004).

S14. I. Bettahi, C. L. Marker, M. I. Roman, K. Wickman, Contribution of the Kir3.1 subunit to the muscarinic-gated atrial potassium channel IKACh. *J Biol Chem* **277**, 48282-8 (2002).